Icarus 206 (2010) 662–668

Contents lists available at ScienceDirect

Icarus

journal homepage: www.elsevier.com/locate/icarus

A bulk cloud parameterization in a Venus General Circulation Model

Christopher Lee [a,*], Stephen R. Lewis [b], Peter L. Read [c]

[a] Division of Geological and Planetary Sciences, California Institute of Technology, 1200 E. California Blvd., M/C 150-21, Pasadena, CA 91125, USA
[b] Department of Physics and Astronomy, The Open University, Walton Hall, Milton Keynes, UK
[c] Department of Physics, University of Oxford, Clarendon Laboratory, Parks Road, Oxford, UK

ARTICLE INFO

Article history:
Received 9 July 2009
Revised 9 September 2009
Accepted 28 September 2009
Available online 13 October 2009

Keyword:
Venus

ABSTRACT

A condensing cloud parameterization is included in a super-rotating Venus General Circulation Model. A parameterization including condensation, evaporation and sedimentation of mono-modal sulfuric acid cloud particles is described. Saturation vapor pressure of sulfuric acid vapor is used to determine cloud formation through instantaneous condensation and destruction through evaporation, while pressure dependent viscosity of a carbon dioxide atmosphere is used to determine sedimentation rates assuming particles fall at their terminal Stokes velocity. Modifications are described to account for the large range of the Reynolds number seen in the Venus atmosphere.

Two GCM experiments initialized with 10 ppm-equivalent of sulfuric acid are integrated for 30 Earth years and the results are discussed with reference to "Y" shaped cloud structures observed on Venus. The GCM is able to produce an analog of the "Y" shaped cloud structure through dynamical processes alone, with contributions from the mean westward wind, the equatorial Kelvin wave, and the mid-latitude/polar Mixed Rossby/Gravity waves. The cloud top height in the GCM decreases from equator to pole and latitudinal gradients of cloud top height are comparable to those observed by Pioneer Venus and Venus Express, and those produced in more complex microphysical models of the sulfur cycle on Venus. Differences between the modeled cloud structures and observations are described and dynamical explanations are suggested for the most prominent differences.

1. Introduction

The atmosphere of Venus has almost complete cloud cover between 40 km and 70 km altitude, dominated by sulfuric acid and water droplets that are thought to come from volcanic out-gassing at the surface (Crumpler et al., 1997). Observations of these cloud layers have indicated significant global scale wave activity (e.g. Del Genio and Rossow, 1990) and planetary scale cloud structures such as the "Y" shaped wave (Esposito et al., 1983). Del Genio and Rossow (1990) analyzed the cloud motions using Pioneer OCPP images (Limaye et al., 1988) and found a number of large scale zonally propagating structures, such as the 5-day Rossby/Mixed-Rossby Gravity (MRG) mode and a 4-day equatorial Kelvin wave.

The microphysical and chemical process in the Venus clouds decks have been investigated in one dimensional models (e.g. Yung and Demore, 1982; Hashimoto and Abe, 2001) but the computational expense of the full sulfur cycle, involving multiple species and interactions, limits their use in current Venus General Circulation Models (GCMs). A number of two dimensional (Yung et al., 2009) and three dimensional circulation models (Yamamoto and Tanaka, 1998) have also been used to investigate the microphysics in the Venus cloud. For example Yamamoto and Tanaka (1998) investigated the production of sulfur oxides by the catalysis reactions of the sulfur oxides and chlorine oxides (SO_x–ClO_x) and suggested that a combination of the Rossby and Kelvin waves are required to reproduce the observed "Y" shaped structure. Yamamoto and Tanaka (1997) prescribed a 4-day wave in a GCM and were able to produce a super-rotating circulation with 5-day Rossby-like waves. The interaction of these two waves produced large scale features analogous to the observed cloud structure.

Yamamoto and Takahashi (2006) included a two-moment microphysical parameterization scheme in their Venus GCM to model the SO_x–ClO_x reaction as well as the water and carbon monoxide interactions with the sulfur compounds. The authors investigated the effect of the meridional circulation on the mass loading and particle distribution of aerosols in the middle atmosphere, and concluded that the aerosol distribution is dominated by the insolation. In the Yamamoto and Takahashi (2006), GCM the meridional circulation equalized the mass loading and fractionated the number concentration by transporting large amounts of small-particle aerosols to the poles in the mean overturning circulation. However, the authors did not comment on the effect of the atmospheric circulation on the formation of cloud structures such as the "Y" shaped wave.

* Corresponding author. Fax: +1 626 585 1917.
E-mail address: lee@gps.caltech.edu (C. Lee).

0019-1035/$ - see front matter © 2009 Elsevier Inc. All rights reserved.
doi:10.1016/j.icarus.2009.09.017

In this study, we use a GCM of the Venus atmosphere, developed at Oxford (Lee et al., 2005, 2007), to investigate the transport of cloud-like passive tracers in the middle atmosphere. In our parameterization of the Venus clouds, we use a simple evaporation/condensation scheme to form clouds from a single volatile source, a sublimation scheme at the surface to provide a source of the volatile and allow the tracers to be advected by the full three dimensional circulation in the atmosphere. The cloud particles were allowed to form instantaneously with no latent heat effects, and fall at their terminal Stokes velocity until they either evaporate or reach the surface. The total mass of volatile in the parameterization is finite and is set at the start of the experiment.

The parameterization scheme we use here includes the simplest possible representation of cloud condensation processes to produce advected condensates within the Venus GCM. We do so in order to investigate the extent to which observed cloud structures on Venus are determined by self-consistent large-scale dynamics alone (unlike the prescribed wave activity in Yamamoto and Tanaka, 1998). This should help clarify the role of more detailed microphysical processes (such as those emphasized by Hashimoto and Abe, 2001, and others).

In the next section we will summarize the main features of the GCM, and describe the cloud condensation parameterization in detail. Following this we present some results from experiments run with the parameterization scheme, and compare the global structures present in the GCM cloud decks with their analogs in the atmosphere of Venus.

2. GCM and cloud parameterization

The Venus GCM developed at Oxford is based on the dynamical core of the Hadley Centre Unified Model (Cullen, 1993); details of the modifications and the parameterization used for the radiative forcing and boundary layer dissipation are given in Lee et al. (2007).

In brief, the physical properties of the planet have been set to values corresponding to Venus (Colin, 1983), such as a mean surface pressure of 9.2 MPa, gravitational acceleration of 8.87 m s^{-1} and a sidereal day length of 243 Earth days. The GCM is configured as an Arakawa B grid (Arakawa and Lamb, 1981) with 5 × 5° resolution in the horizontal, and 33 levels extending from the surface to 90 km altitude, with a maximum vertical grid spacing of 3.5 km.

The radiative forcing of the GCM is parameterized using a linearized "Newtonian" relaxation (or "cooling-to-space") towards the observed temperature profile derived from Pioneer Venus probe data (Seiff et al., 1980), and a vertical heating profile is used to simulate the radiative effect of a middle atmosphere cloud deck and optically thick lower atmosphere. The planetary boundary layer is parameterized by a bulk transport turbulent mixing scheme (Jacobson, 2005) over flat orography with constant assumed roughness with a roughness length of 0.03 m, corresponding to a sparsely bouldered surface.

This simplified model configuration produces significant superrotation in the atmosphere without specific or excessive forcing, but does not so far reproduce in quantitative detail the high westward wind speeds observed in the upper atmosphere (Seiff, 1983; Del Genio and Rossow, 1990). The GCM reproduces the basic structure of the atmospheric circulation, including a mid-latitude Rossby wave and an equatorial Kelvin wave, albeit with periods of 30 days and 9.5 days, compared to 5 days and 4 days for the observed modes (Del Genio and Rossow, 1990), respectively. The peak equatorial wind speeds in a typical experiment with the GCM are 50 m s^{-1} compared to over 100 m s^{-1} derived from Pioneer Venus observations of Venus (Seiff, 1983). Mean westward winds on the equator peak at 35 m s^{-1} in the GCM. The mean westward wind speeds and wave frequencies are both reduced by approximately the same amount relative to the observed wind speeds and wave frequencies. Fig. 1 shows the time and longitudinal mean westward wind in this GCM for an experiment including the cloud parameterization, averaged over 300 Earth days with 1 day sampling (chosen to sample multiple periods of the planetary scale waves). Also shown in Fig. 1 is the deviation of time and longitudinal mean temperature from the global mean temperature profile $T(z)$. This temperature 'anomaly' shows the warm pole feature at 5 kPa and a cold pole at 500 kPa, bounding the bulk of the westward jet.

Within this GCM, we have implemented a passive cloud tracer model to allow tracers to be advected by the atmospheric circulation in the middle atmosphere. The model is based on a sulfuric

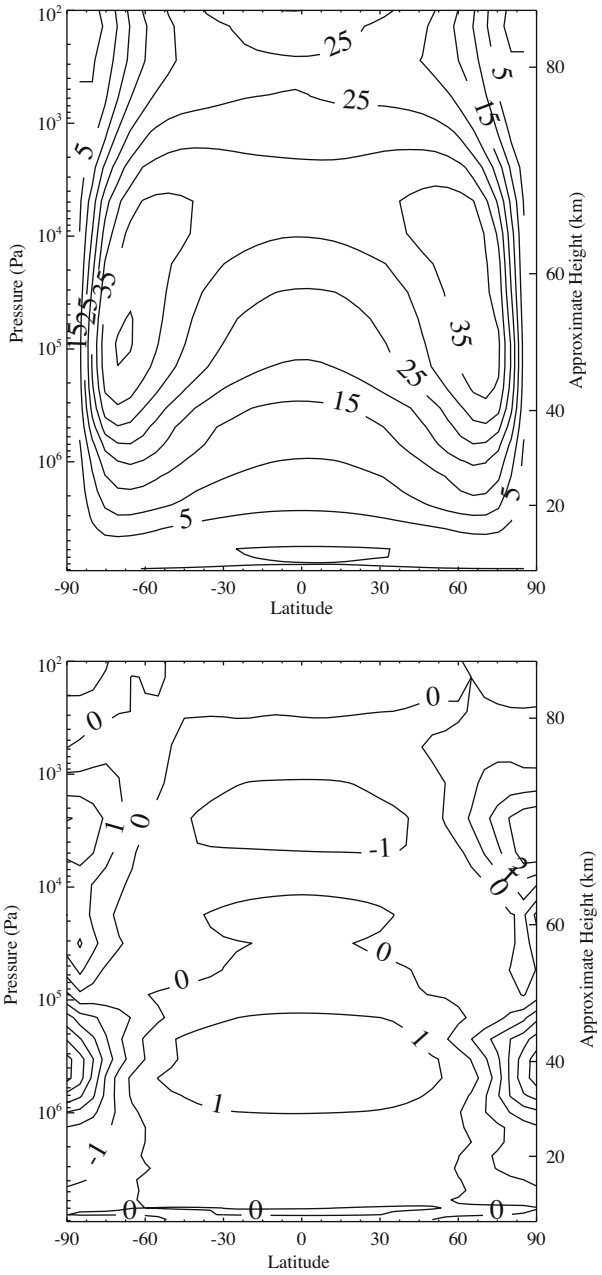

Fig. 1. (top) Time and zonal mean westward wind, for the GCM described here and in Lee et al. (2007), for the experiment discussed here including the passive cloud parameterization, contour interval of 5 m s^{-1}. (bottom) Time mean temperature anomaly ($\overline{T - T(z)}$) for the same experiment, contour interval of 1 K.

acid cycle (Hashimoto and Abe, 2001) but does not include any explicit creation or destruction processes. Instead we assume that the surface acts as a reservoir for the sulfuric acid liquid (or a chemical precursor), which is allowed to evaporate into the atmosphere if the lowest layer is sub-saturated. The saturation vapor pressure (SVP) is assumed to be that of sulfuric acid and is a function of temperature only. Using this method, we are able to investigate the transport of cloud particles by the atmospheric circulation without the full complications of chemical and radiative feedback.

The flux of tracer volatile from the surface is given by a simple bulk drag law,

$$F = -C_H|u_1|(q_1 - q_{\mathrm{sat}}(T)), \tag{1}$$

where u_1 is the wind speed in the boundary layer, q_1 is the mass mixing ratio of the volatile in the boundary layer, and q_{sat} is the saturation mixing ratio for the volatile as a function of temperature. C_H is the bulk heat-transfer coefficient (the Stanton number, Jacobson, 2005), derived using the Monin–Obukhov similarity theory (Monin and Obukhov, 1954) within the planetary boundary layer of the GCM.

Once in the atmosphere, the volatile condenses (evaporates) in super-saturated (sub-saturated) air and is advected by the three dimensional wind field of the GCM. In the cloud-liquid phase, the volatile has an additional sublimation/precipitation process whereby the cloud particles drop at their terminal Stokes velocity until they reach a sub-saturated air parcel, or they reach the surface as 'rain'. In practice, it does not 'rain' on the surface because the atmosphere is generally unsaturated below 50 km, and all cloud particles evaporate below this level.

The terminal Stokes velocity of the liquid particles is given by

$$V_z = \frac{2r_p^2\rho_p}{9\mu}C_n g, \tag{2}$$

where r_p is the particle radius, assumed here to be the 1 μm 'Mode 2' particles (Esposito et al., 1997) and ρ_p is the particle density, assumed to be 1800 kg m^{-3} (the density of sulfuric acid at STP (Lide, 1995)). g is the gravitational acceleration of Venus, 8.87 m s^{-1}, μ is the viscosity of carbon dioxide, and C_n is the Cunningham slip correction factor (Rossow, 1978).

The viscosity of carbon dioxide, μ, is assumed to be a function of atmospheric temperature only (Lide, 1995; Reid et al., 1987).

$$\mu = \frac{807x^{0.618} - 357e^{-0.449x} + 340e^{-4.058x} + 18}{176\left(\frac{T_c}{m^3P_c^4}\right)^6}, \tag{3}$$

where $x = T/T_c$, T_c is the critical temperature (304.1 K), P_c is the critical pressure (7.38 MPa), and m is the molecular mass of carbon dioxide.

The Cunningham slip correction factor, extends the Stokes approximation from the surface (where the Reynolds number is approximately 1) to 80 km altitude (an atmospheric pressure of about 500 Pa, where the free path length in the gas and the particle radius are equal $\lambda_r \simeq r_p$). The Cunningham slip correction factor is given by

$$\begin{aligned} C_n &= 1 + \frac{4}{3}K_n, \\ &= 1 + \frac{4}{3}\frac{\lambda_p}{r_p}, \end{aligned} \tag{4}$$

where K_n is the Knudsen number, λ_p is the mean free path, and r_p is the radius of the particle.

However, the Stokes velocity is insignificant compared to the typical vertical winds throughout most of the atmosphere (about 1×10^{-9} mm s^{-1} compared to 1 mm s^{-1}) and the motion of volatile material is dominated by advection. The important exception to this situation is that where the vertical velocity is zero, such as at the top of the overturning cell and at all heights between the upward and downward branches of the cell, the Stokes flow becomes dominant. Fig. 2 is a schematic of this model and shows the sources and sinks of each component in the simplified cloud model, together with the possible transfers between each state.

3. Results

Two GCM experiments were initialized with extreme distributions of a cloud-like tracer. In the first experiment, 0.5 precipitable-mm of tracer was placed at the surface as liquid, corresponding to 10 parts-per-million by volume (ppmv) of well-mixed gaseous volatile (Esposito et al., 1997; Jenkins et al., 1994). In the second experiment, the same total mass of volatile was placed as a liquid cloud deck at 40–50 km with global coverage. Both experiments were initialized with the same statistically steady atmospheric circulation previously integrated for 23,000 days, and integrated for a further 7320 days to allow the volatile to distribute throughout the atmosphere.

The global and time averaged vertical profile of the volatile in the atmosphere was found to be approximately the same in both cases, as shown in Fig. 3. In both experiments, the clouds form above 50 km where the saturation vapor pressure exceeds the atmospheric pressure. However, the decreasing net upward mass flux of the volatile results in 90% of the cloud liquid mass being confined between 50 km and 65 km in both experiments (66% of the cloud liquid accumulated in the 50–55 km layer in both models).

No clouds were found to form below the 'cloud base' at 50 km and the air is permanently sub-saturated below the base. However, the predicted volume mixing ratio (VMR) of sulfuric acid of 10 ppmv is not a realistic value for the amount of gaseous sulfuric acid in the lower Venus atmosphere, where it would be decomposed into oxides of sulfur and water (Hashimoto and Abe, 2001). The qualitative result from the volatile distribution in the lower atmosphere is that the lower atmosphere appears well-mixed after 7320 days (30 Venus years). The upper atmosphere differs between the two experiments because the initial distributions were significantly different, and the upper atmosphere has not fully equilibrated within the integration. A surface reservoir of 0.75 kg m^{-2} (~2 ppmv equivalent) of liquid exists on the surface, with a minimum of half this value on the equator because of upwelling in this region.

The horizontal structure of the clouds varies significantly under the influence of the atmospheric circulation and the temperature variation at the altitude of the cloud deck. A peak cloud liquid concentration of ~8.5 ppmv occurs on the equator at 55–60 km, which

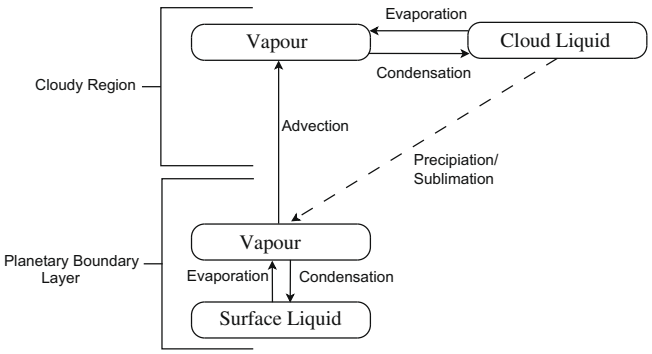

Fig. 2. Schematic of the cloud tracer parameterization. The dashed line indicates a process that is possible but is not significant in this model. Planetary Boundary Layer (PBL) flux only occurs in the lowest model layer.

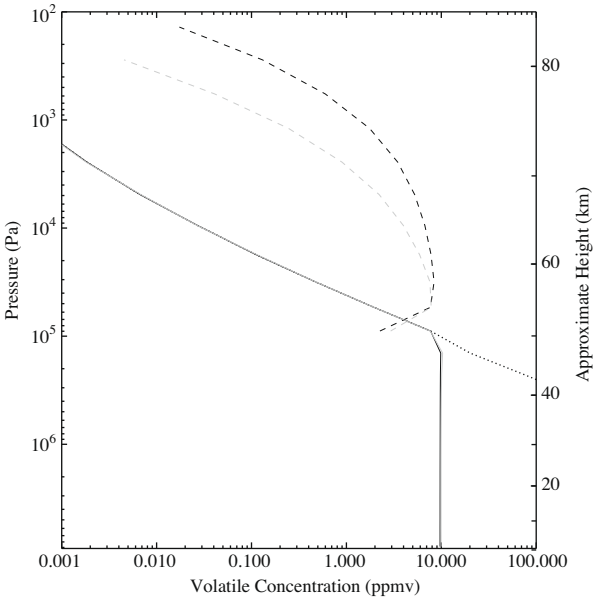

Fig. 3. Global and time average volatile concentration in the two experiments. Solid lines show the vapor concentration, black for the experiment initialized with volatile at the surface, gray for the experiment initialized with cloud volatile (the lines overlap almost entirely). The vapor concentration is bounded by the saturation vapor pressure (dotted line) that is overlapped below ~10 ppm. The dashed lines show the cloud concentration for the same experiments.

decreases by 2 ppm to ~6.5 ppmv (~25% reduction near both poles). For comparison, Yamamoto and Takahashi (2006) show a mass loading (Fig. 9 in Yamamoto and Takahashi, 2006) variation of 40% and number concentration (Fig. 6 in Yamamoto and Takahashi, 2006) variation of 25% in the same region of the atmosphere, as a function of latitude. In the vapor phase, a similar latitudinal gradient is found at 50–55 km, where the volatile concentration drops from ~8 ppmv at the equator to ~6 ppmv at the pole. The polar regions have a combination of colder air and less total volatile, which results in lower amounts of cloud volatile. Fig. 4 shows the time and longitudinal mean cloud liquid and vapor concentration for the experiment initialized with surface liquid (also averaged over 300 days with 1 day sampling).

Fig. 4 also shows the mean Eulerian streamfunction for this experiment. Most of the mass transport within the meridional cell in the GCM does not extend above about 60 km, near the peak of the clouds. The Newtonian relaxation profile used in this GCM likely forces a lower atmosphere meridional circulation which is somewhat stronger than the observed circulation. However, the cloud structure is more dependent on the location of the top of the meridional cell, which depends on the location of the peak of the solar forcing in the atmosphere, not on the details of the lower atmosphere circulation. The peak of the solar forcing in the model is derived from flux and temperature observations of the atmosphere of Venus, which in turn depend on the cloud structure. It is not surprising, therefore, that the cloud maximum in the GCM occurs near the observed altitude.

A reduction in polar cloud was observed by Pioneer Venus (Esposito et al., 1983) as a region of increased brightness temperature because the reduced cloud optical depth allows more radiation to escape from the hot lower atmosphere. Esposito et al. (1983) suggest that the "cloud top" height drops from ~50 mb (5 kPa, 65 km) to ~125 mb (12.5 kPa, 60 km), where the cloud top corresponds to where the cloud density falls to approximately 100 particles/cm^2, or approximately 4–5 ppmv. In the experiment shown in Fig. 4, the 5–6 ppmv cloud liquid contour is closest to the "cloud top" pressures at the equator and pole, although in this

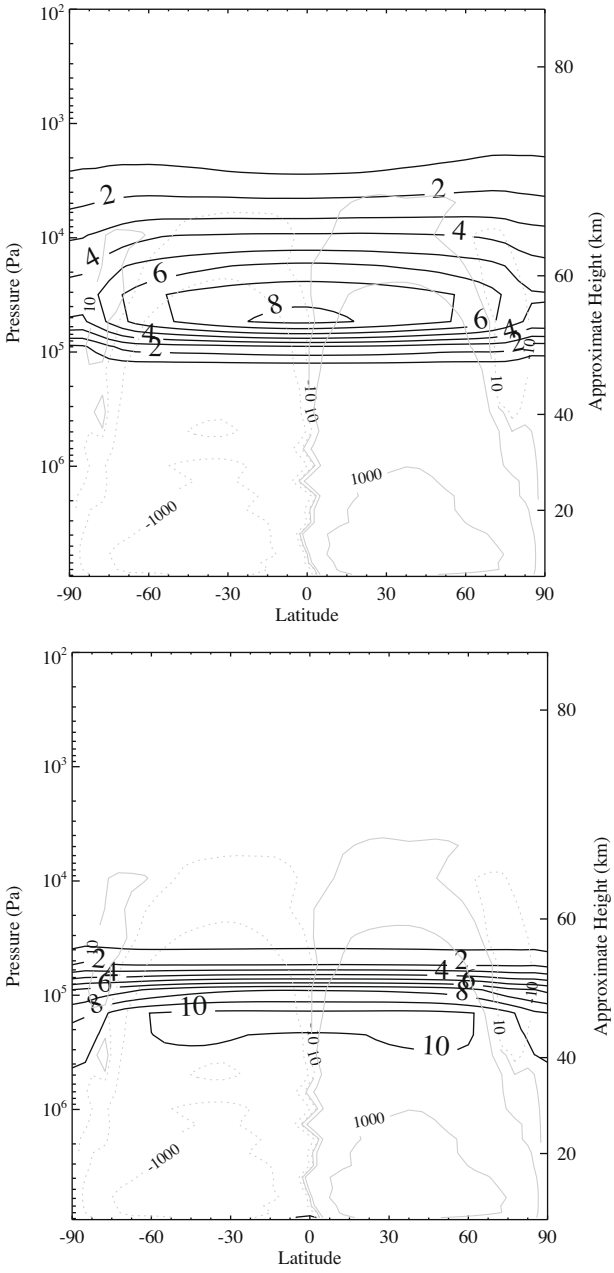

Fig. 4. Time and longitudinal mean vapor concentration (top figure) and cloud liquid concentration (bottom figure) for the experiment initialized with surface liquid. Contour intervals are 1 ppmv from 0 ppmv. Light gray contours indicate Eulerian streamlines at 10 Tg/s, 100 Tg/s, and 1000 Tg/s clockwise (solid) and counter-clockwise (dashed).

experiment the decrease occurs over a larger latitude range than in the observed cloud deck. This is a consequence of assuming a single particle type and radius in this experiment. Similar results were found by Titov et al. (2008), where the observations indicate a cloud top decrease of 8 km (from 72 km to 64 km) from equator to pole.

Where the volatile does not change state rapidly, its mixing ratio behaves as a passive tracer for the atmospheric circulation in both liquid and vapor phases. The global structure is then controlled by a combination of the mean circulation and motions of both the mid-latitude Rossby wave and the equatorial Kelvin wave. Fig. 5 shows several snapshots of the clouds at 55 km showing the various shapes produced by the clouds due to the atmospheric circulation. In a number of the subplots, the Kelvin and Rossby waves

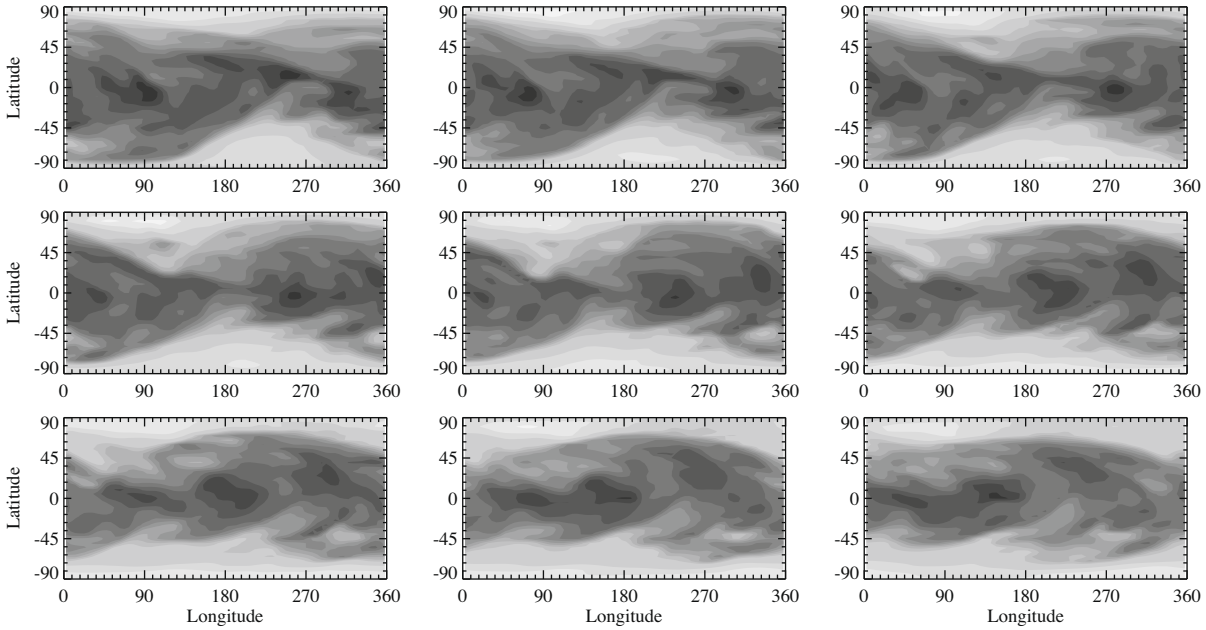

Fig. 5. Snapshots of the cloud-deck at 55 km for nine consecutive days (left to right, then top to bottom), showing a propagating large scale feature reminiscent of the Y-shape cloud structure on Venus. Dark shading represents higher concentrations of cloud liquid. Contour shades are not linear and have been modified to de-emphasize the poles and emphasize the mid-latitudes.

interact to produce shapes analogous to the observed horizontal "Y" shape, albeit somewhat smoothed by the coarse resolution of the GCM.

In Fig. 5, the horizontally aligned "Y" structure moves from right to left (in the direction of the mean zonal wind) and maintains its large scale structure over a period of about 7 days, which is a significant fraction of the period of the MRG wave. The coherence time of the structure in the GCM may be a result of the 'beat pattern' produced by the interaction of the equatorial and mid-latitude waves in the GCM. In this experiment, the equatorial waves are three times faster than the mid-latitude waves and would produce a relatively high frequency 'beat pattern', reducing the coherence time. More closely matched wave periods (Del Genio and Rossow, 1990) would tend to have lower frequency 'beat patterns', and thus longer coherence timescales.

Fig. 6 shows a similar sequence of 4 days taken over the south pole of the same experiment. In this view the cloud decks appear as a vortex structure (Taylor et al., 1983) with multiple 'arms' extending from the polar region. The polar vortex itself is situated away from the pole and slowly processes around the south pole. The same type of structure can be seen in the northern hemisphere, and in this experiment the formation and shedding of the 'arms' appears to be random in time.

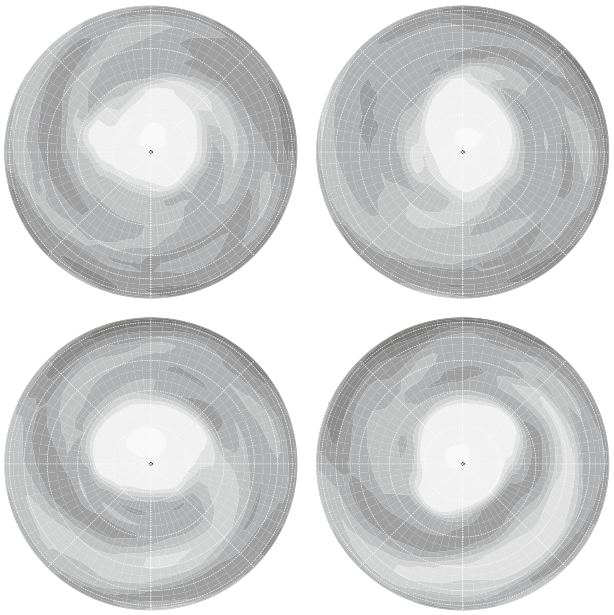

Fig. 6. Snapshots of the cloud-deck at 55 km for four consecutive days (left to right, then top to bottom) taken over the south pole, showing a large vortex structure rotating around the south pole in the direction of the mean zonal wind. Dark shading represents higher concentrations of cloud liquid. Contour shades are not linear and have been modified to emphasize the 'arms' of the polar vortex.

4. Conclusions

During the development of a Venus GCM with a super-rotating circulation, we have implemented a passive cloud condensation scheme to investigate the cloud structures produced by the circulation and eddy transport in the middle atmosphere of Venus.

Although we use a much simplified parameterization of the chemical processes in the sulfur cycle, we find that a parameterization based solely on the SVP of sulfuric acid is sufficient to form clouds at approximately the observed temperature and pressure range in the GCM. The mean winds and planetary scale waves that exist at this altitude are sufficient to produce organized cloud structures that look remarkably similar to the striking features of the Venus clouds. These results also agree with recent observations from Venus Express (Titov et al., 2008; Ignatiev et al., 2009), although the work presented here was performed before the launch of Venus Express.

The "Y" shaped features in the GCM has a short coherence time, typically of a few days, which may be shorter than the observed coherence time in the Venus clouds. The feature also appears to be more symmetric about the equator in many observations Moissl et al. (2009) than in the GCM. The latter difference may be explained by the lack of a diurnal tide in the GCM. In similar experiments where a diurnal tide was applied to the heating profile

(but clouds were disabled), the GCM atmosphere responds to the symmetric tidal forcing by developing symmetric Rossby-like waves instead of asymmetric MRG-like waves observed in this experiment. A similar effect is presented in Yamamoto and Takahashi (2003, 2004). This change in the eddy temperature structure is likely to affect the eddy driven cloud structure that appears as a global "Y" shape.

The long coherence time in observations is more difficult to explain, but it may be a result of the relative wave and wind speeds present in the cloud region. In the model, the equatorial waves propagate westward three times faster than the polar waves, and the cloud structure has a 'beat pattern' with a short period resulting from the interference of the propagating wave modes. In the atmosphere of Venus, the equatorial wave period is similar to the polar wave period (within about 20%), resulting in a much longer 'beat' period in the corresponding interference pattern.

The similarity between clouds found in the observations and the GCM show that the atmospheric circulation is a major driver of the structures observed in the clouds (as suggested by Del Genio and Rossow, 1990; Schinder et al., 1990; Suomi and Limaye, 1978) and reinforce their use as observational proxies for the winds within the clouds. Over periods of a few hours, the horizontal winds will clearly dominate other processes, except in the most convective or chemically active regions.

Observations by Venus Express have recently been used to derive westward wind speeds within the Venus cloud decks which show little change between the Pioneer Venus (Del Genio and Rossow, 1990) to the Galileo (Carlson et al., 1991) and Venus Express (Moissl et al., 2009) missions spanning two decades. This suggests that the middle atmosphere super-rotation is a long-lasting feature of the Venus atmosphere, and that the waves are also a persistent, coherent and regular feature of the circulation.

The structure of the polar dipole and cold collar in the GCM does not agree with the observations (Schofield and Taylor, 1983; Titov et al., 2008; Ignatiev et al., 2009). The fine structured polar dipole does not appear in the GCM, instead a wavenumber 2 is present in the form of an elliptical temperature minimum at the pole, and the cold collar temperature minimum is weaker in the GCM (about 10 K) compared to observations (about 40 K), while being larger in horizontal extent in the GCM. Both of these features might be better resolved in a simulation with a higher horizontal resolution if they are dominated by dynamical effects. It is possible that microphysics enhances the depth of the temperature minimum, but no model has been suggested that would produce such an extreme effect.

The lack of microphysics, as well as sub-gridscale convection, means that the GCM does not simulate the influx of the cloud particles at the cloud base. Titov et al. (2008) suggest that small scale convective activity in the equatorial regions brings large amounts of the UV absorber into the cloud decks, while the low temperature lapse rate in the polar region inhibits its loss from the collar and enhances the cloud concentration there. An improved microphysical scheme is relatively straightforward to implement in the framework provided by the HadAM3 GCM, but at significant computational expense. However, simulating the small scale convection explicitly is not possible without a prohibitively high horizontal resolution. A better solution would be to employ a sub-gridscale parameterization using Convective Available Potential Energy (CAPE) to determine the amount of convection (Jacobson, 2005).

Acknowledgments

This work was funded by a PPARC studentship (C. Lee). The authors thank the UK Meteorological Office for the use of the HadAM3 climate model in this work and Henning Böttger for the cloud parameterization upon which the Venus cloud model used in this work is based. We thank the two anonymous reviewers for their useful comments and corrections.

References

Arakawa, A., Lamb, V.R., 1981. A potential enstrophy and energy conserving scheme for the shallow water equations. Mon. Weather Rev. 109, 18–36.
Carlson, R.W., and 20 colleagues, 1991. Galileo infrared imaging spectroscopy measurements at Venus. Nature 253 (5207), 1541–1548.
Colin, L., 1983. Basic facts about Venus. In: Bougher, S.W., Hunten, D.M., Phillips, R.J. (Eds.), Venus II. The University of Arizona Press, Tucson, pp. 10–26.
Crumpler, L.S., Aubele, J.C., Senske, D.A., Keddie, S.T., Magee, K.P., Head, J.W., 1997. Volcanoes and centres of volcanism on Venus. In: Bougher, S.W., Hunten, D.M., Phillips, R.J. (Eds.), Venus II. The University of Arizona Press, Tucson, pp. 97–756.
Cullen, M.J.P., 1993. The unified forecast climate model. Meteorol. Mag. 122, 81–94.
Del Genio, A.D., Rossow, W.B., 1990. Planetary-scale waves and the cyclic nature of cloud top dynamics on Venus. J. Atmos. Sci. 47, 293–318.
Esposito, L.W., Bertaux, J.-L., Krasnoplosky, V., Moroz, V.I., Zasova, L.V., 1983. The clouds and hazes of Venus. In: Hunten, D.M., Colin, L., Donahue, T.M., Moroz, V.I. (Eds.), Venus. The University of Arizona Press, Tucson, pp. 484–564.
Esposito, L.W., Bertaux, J.-L., Krasnoplosky, V., Moroz, V.I., Zasova, L.V., 1997. Chemistry of lower atmosphere and clouds. In: Bougher, S.W., Hunten, D.M., Phillips, R.J. (Eds.), Venus II, pp. 415–458.
Hashimoto, G.L., Abe, Y., 2001. Predictions of simple cloud model for water vapour cloud albedo feedback on Venus. J. Geophys. Res. 106, 14675–14690.
Ignatiev, N.I., Titov, D.V., Piccioni, G., Drossart, P., Markiewicz, W.J., Cottini, V., Roatsch, Th., Almeida, M., Manoel, N., 2009. Altimetry of the Venus cloud tops from the Venus Express observations. J. Geophys. Res. 114, E00B43. doi:10.1029/2008JE003320.
Jacobson, M.Z., 2005. Fundamentals of Atmospheric Modelling. Cambridge University Press, Cambridge.
Jenkins, J.M., Steffes, P.G., Hinson, D.P., Twicken, J.D., Tyler, G.L., 1994. Radio occultation studies of the Venus atmosphere with the Magellan Spacecraft. 2. Results from the October-1991 Experiments. Icarus 110 (1), 79–94.
Lee, C., Lewis, S.R., Read, P.L., 2005. A numerical model of the atmosphere of Venus. Adv. Space Res. 6 (11), 2142–2145.
Lee, C., Lewis, S.R., Read, P.L., 2007. Superrotation in a Venus general circulation model. J. Geophys. Res. 112 (E4), E04S11.
Lide, D.R. (Ed.), 1995. Handbook of Chemistry and Physics. CRC Press.
Limaye, S.S., Grassoti, C., Kuetemeyer, M.J., 1988. Venus: Cloud level circulation during 1982 as determined from Pioneer photopolarimeter images. Part 1: Time and zonally averaged circulation. Icarus 73, 193–211.
Moissl, R., and 12 colleagues, 2009. Venus cloud top winds from tracking UV features in Venus monitoring camera images. J. Geophys. Res. doi:10.1029/2008JE003117.
Monin, A.S., Obukhov, A.M., 1954. Basic laws of turbulent mixing in the ground layer of the atmosphere. Trans. Geophys. Inst. Akad. Nuak. 151, 1963–1987.
Reid, R.C., Prausnitz, J.M., Poling, B.E., 1987. The Properties of Gases and Liquids, fourth ed. McGraw Hill, New York, USA. pp. 1–741. ISBN:0-07-051799-1.
Rossow, W.B., 1978. Cloud microphysics: Analysis of the clouds of Earth, Venus, Mars and Jupiter. Icarus 36, 1–50.
Schinder, P.J., Gierasch, P.J., Leroy, S.S., Smith, M.D., 1990. Waves, advection, and cloud patterns on Venus. J. Atmos. Sci. 47, 2037–2052.
Schofield, J.T., Taylor, F.W., 1983. Measurements of the mean, solar-fixed temperature and cloud structure of the middle atmosphere of Venus. Q. J. R. Meteorol. Soc. 109 (459), 57–80.
Seiff, A., 1983. Thermal structure of the atmosphere of Venus. In: Hunten, D.M., Colin, L., Donahue, T.M., Moroz, V.I. (Eds.), Venus. The University of Arizona Press, Tucson, pp. 15–279.
Seiff, A., Kirk, D.B., Young, R.E., Blanchard, R.C., Findlay, J.R., Kelly, G.M., Sommer, S.C., 1980. Measurements of thermal structure and thermal contrasts in the atmosphere of Venus and related dynamics observations: Results from the four Pioneer Venus probes. J. Geophys. Res. 85, 7903–7933.
Suomi, V.E., Limaye, S.S., 1978. Further evidence of vortex circulation. Science 201, 1009–1011.
Taylor, F.W., Hunten, D.M., Ksanfomaliti, L.V., 1983. The thermal balance of the middle and upper atmosphere of Venus. In: Hunten, D.M., Colin, L., Donahue, T.M., Moroz, V.I. (Eds.), Venus. The University of Arizona Press, Tucson, pp. 650–680.
Titov, D.V., Taylor, F.W., Svedhem, H., Ignatiev, N.I., Markiewicz, W.J., Piccioni, G., Drossart, P., 2008. Atmospheric structure and dynamics as the cause of ultraviolet marking in the clouds of Venus. Nature 456, 620–623.
Yamamoto, M., Takahashi, M., 2003. The fully developed superrotation simulated by a general circulation model of a Venus-like atmosphere. J. Atmos. Sci. 60 (3), 561–574.
Yamamoto, M., Takahashi, M., 2004. Dynamics of Venus' superrotation: The eddy momentum transport processes newly found in a GCM. Geophys. Res. Lett. 31 (9), L09701.
Yamamoto, M., Takahashi, M., 2006. An aerosol transport model based on a two-moment microphysical parameterization in the Venus middle atmosphere: Model description and preliminary experiments. J. Geophys. Res. 111, E08002.
Yamamoto, M., Tanaka, H., 1997. Formations and maintenance of the 4-day circulation in the Venus middle atmosphere. J. Atmos. Sci. 54, 1472–1489.

Yamamoto, M., Tanaka, H., 1998. The Venusian Y-shaped cloud pattern based on aerosol-transport model formations and maintenance of the 4-day circulation in the Venus middle atmosphere. J. Atmos. Sci. 55, 1400–1416.
Yung, Y.L., Demore, W.B., 1982. Photochemistry of the stratosphere of Venus: Implications for atmosphere evolution. Icarus 51, 199–247.
Yung, Y.L., Liang, M.V., Jiang, X., Schia, R.L., Lee, C., Bezard, B., Marcq, E., 2009. Evidence for carbonyl sulfide (OCS) conversion to CO in the lower atmosphere of Venus. J. Geophys. Res. 114. doi:10.1029/2008JE003094.